Lanczos Algorithm, the Transfer Matrix, and the Signal-to-Noise Problem

Michael L. Wagman
Fermi National Accelerator Laboratory, Batavia, Illinois 60510, USA

(Received 3 September 2024; revised 23 April 2025; accepted 7 May 2025; published 17 June 2025)

This Letter introduces a method for determining the energy spectrum of lattice quantum chromodynamics by applying the Lanczos algorithm to the transfer matrix and using a bootstrap generalization of the Cullum-Willoughby method to filter out spurious eigenvalues. Proof-of-principle analyses of the simple harmonic oscillator and the lattice quantum chromodynamics proton mass demonstrate that this method provides faster ground-state convergence than the "effective mass," which is related to the power-iteration algorithm. Lanczos provides more accurate energy estimates than multistate fits to correlation functions with small imaginary times while achieving comparable statistical precision. Two-sided error bounds are computed for Lanczos results and guarantee that excited-state effects cannot shift Lanczos results far outside their statistical uncertainties.

DOI: 10.1103/pcvc-734h

Determining the energy spectrum of quantum chromodynamics (QCD) leads to hadron mass predictions and is an essential first step toward predicting hadron and nuclear structure, scattering amplitudes, and inputs to new physics searches. Spectroscopy, the determination of ground- and excited-state energies, is therefore a central aspect of lattice QCD (LQCD) calculations. Accurately disentangling ground- and excited-state effects is challenging for systems with small energy gaps and leads to significant and hard-to-quantify uncertainties in state-of-the-art LQCD calculations, for example, of nucleon axial form factors [1–8] and baryon-baryon scattering [9–13].

Spectroscopy calculations typically rely on analyzing the asymptotic decay rate of Euclidean correlation functions, which is set by the lowest-energy state not orthogonal to those created by the relevant operators. However, the signal-to-noise ratios (SNRs) of Euclidean correlation functions also decay exponentially in Euclidean time with a rate predicted by Parisi and Lepage [14,15]. This so-called SNR problem is a major challenge for proton and other baryon correlation functions and becomes exponentially more severe for nuclei [16–18].

The SNR problem has motivated the development of methods to maximize the information that can be extracted from relatively precise correlation functions with small imaginary times. Techniques based on solving a generalized eigenvalue problem constructed from a symmetric correlation-function matrix provide both faster convergence and rigorous variational upper bounds on energies [19–23], and their application has become standard in LQCD spectroscopy for multihadron systems with small energy gaps [24–26]. Prony's method for signal processing has also been applied to LQCD and shown to improve ground-state convergence [27–31].

This Letter proposes a new approach to LQCD spectroscopy using the Lanczos algorithm [32] to compute eigenvalues of the transfer matrix. The Lanczos algorithm has been widely applied for decades to computational linear algebra [33–39], quantum Monte Carlo calculations [40–42], and analysis of Dirac matrices in LQCD [43–49]. However, direct application of the Lanczos algorithm to the LQCD transfer matrix is challenging because the transfer matrix is infinite-dimensional [50] and not directly constructed in path-integral Monte Carlo calculations.

Here, I show that the Lanczos algorithm can be applied to the LQCD transfer matrix using recursive formulas whose inputs are simply Euclidean correlation functions. The Kaniel-Paige-Saad (KPS) bound [51–53] implies that Lanczos energies converge exponentially faster than standard estimators near the continuum limit. Lanczos approximation errors can be estimated directly and provide two-sided error bounds, improving upon the one-sided variational bounds provided by generalized eigenvalue problem solutions.

Proof-of-principle results are shown below for a quantum simple harmonic oscillator and the proton mass in LQCD with close-to-physical quark masses. The variance of Lanczos estimators is found to approach a constant for large iteration counts, in contrast to algebraic estimators based on "effective masses" whose variance grows exponentially in accordance with Parisi-Lepage scaling. An explanation for this behavior is proposed based on the identification of Lanczos as a Krylov-space projection

Published by the American Physical Society under the terms of the Creative Commons Attribution 4.0 International license. Further distribution of this work must maintain attribution to the author(s) and the published article's title, journal citation, and DOI. Funded by SCOAP³.

method and analysis of projection operator SNRs inspired by Della Morte and Giusti [54–56]. Of course, extending the maximum time included in a multistate fit offers the same improvement. Unlike fits, however, Lanczos results are purely algebraic functions of LQCD "data" and do not require any statistical inference, cuts on what subset of data is included, Bayesian priors, or covariance-matrix estimation. In examples where only small ranges of data are available, Lanczos results simultaneously achieve similar variance and less bias than multistate fit results.

Method—Lattice field theories do not have a continuous time-translation symmetry to be used to directly define a Hamiltonian operator H. The presence of discrete time-translation symmetry, $t \to t + a$, where a is the lattice spacing, does allow a transfer matrix $T = e^{-aH}$ to be defined that acts as an imaginary-time evolution operator. The transfer matrix for LQCD with the Wilson gauge and fermion actions has been explicitly constructed as a Hilbert-space operator and shown to be Hermitian and positive-definite [57]. A transfer matrix can also be constructed for theories with improved actions that acts as a positive-definite operator for low-energy states [58].

Euclidean correlation functions for a theory with temporal extent (inverse temperature) β and "interpolating operators" ψ and $\psi^\dagger$ are matrix elements of powers of T,

$$C(t) \equiv \langle \psi(t)\psi^\dagger(0)\rangle = \langle \psi|T^{t/a}|\psi\rangle + \ldots, \tag{1}$$

where $|\psi\rangle \equiv \psi^\dagger|0\rangle$ with $|0\rangle$ the vacuum state and ... denotes thermal effects detailed in Supplemental Material [59], which also includes Refs. [60,61]. Inserting complete sets of transfer-matrix eigenstates $\sum_n |n\rangle\langle n|$ leads to the spectral representation

$$C(t) = \sum_n \lambda_n^t \langle\psi|n\rangle\langle n|\psi\rangle = \sum_{n=0}^{\infty} |Z_n|^2 e^{-E_n t}, \tag{2}$$

where $Z_n \equiv \langle n|\psi\rangle$ are overlap factors. Energies are defined by $E_n \equiv -(1/a)\ln\lambda_n$ in terms of transfer matrix eigenvalues $\lambda_n \equiv \langle n|T|n\rangle$ in the sector with quantum numbers of $\psi^\dagger|0\rangle$ ordered such that $\lambda_0 \geq \lambda_1 \geq \ldots$. For large t, correlation functions are dominated by contributions from the lowest-energy state that is not orthogonal to $|\psi\rangle$. The "effective mass" is an algebraic estimator for the ground-state energy

$$E(t) \equiv -\frac{1}{a}\ln\left[\frac{C(t)}{C(t-a)}\right] = E_0 + O\left(e^{-(t/a)\delta}\right), \tag{3}$$

where $\delta \equiv a(E_1 - E_0)$ is the excitation gap.

Estimating the ground-state energy using the effective mass can be viewed as an application of the power-iteration method [62] to the transfer matrix as follows. This method defines $|b_k\rangle \equiv T|b_{k-1}\rangle/||T|b_{k-1}\rangle||$ with $|b_1\rangle = |\psi\rangle/\sqrt{\langle\psi|\psi\rangle}$, which leads to $|b_k\rangle \propto T^{k-1}|\psi\rangle$. For Hermitian T, the Hilbert-space norm satisfies $||T|\psi\rangle|| = \langle\psi|T^2|\psi\rangle = C(2a)$. The largest eigenvalue of T is then approximated as

$$\mu_k \equiv \frac{\langle b_k|T|b_k\rangle}{\langle b_k|b_k\rangle} = \frac{\langle\psi|T^{2k-1}|\psi\rangle}{\langle\psi|T^{2(k-1)}|\psi\rangle} = \frac{C((2k-1)a)}{C((2k-2)a)}. \tag{4}$$

Taking the log gives the power-iteration energy estimate after k iterations: $-(1/a)\ln\mu_k$. This estimate is identical to the effective mass with $t/a = 2k - 1$.

The Lanczos algorithm [32] is widely appreciated to be superior to the power-iteration method for the task of approximating the largest eigenvalue of a matrix [33–38,63–66]. Both methods involve the Krylov space

$$\mathcal{K}^{(m)} = \text{span}\{|\psi\rangle, T|\psi\rangle, \ldots, T^m|\psi\rangle\}, \tag{5}$$

and the approximation of eigenvectors as elements of $\mathcal{K}^{(m)}$. However, the Lanczos algorithm enables the explicit diagonalization of a Krylov-space approximation to T that leads to faster convergence as discussed below. Lanczos vectors are defined by the three-term recurrence

$$T|v_j\rangle = \alpha_j|v_j\rangle + \beta_j|v_{j-1}\rangle + \beta_{j+1}|v_{j+1}\rangle. \tag{6}$$

This guarantees that $\langle v_i|v_j\rangle = \delta_{ij}$ and therefore $\{|v_1\rangle, \ldots, |v_m\rangle\}$ provides an orthonormal basis for $\mathcal{K}^{(m)}$. The matrix elements of T in this basis, $T_{ij}^{(m)} \equiv \langle v_i|T|v_j\rangle$, form a tridiagonal matrix by Eq. (6). Its eigenvalues $\lambda_n^{(m)}$, called "Ritz values," provide optimal Krylov-space approximations to eigenvalues of T [33].

The LQCD transfer matrix is an infinite-dimensional integral operator that cannot be explicitly represented numerically without some form of Hilbert-space truncation. However, the elements of $T_{ij}^{(m)}$ are scalars constructed from inner products involving $|\psi\rangle$ and T. The path-integral definitions of $T_{ij}^{(m)}$ can be related to those for Euclidean correlation functions $C(ka)$ by defining normalized states $|v_1\rangle = |\psi\rangle/\sqrt{\langle\psi|\psi\rangle}$, as in the first step of the power-iteration method, and matrix elements $A_j^{(p)} \equiv \langle v_j|T^p|v_j\rangle$ and $B_j^{(p)} \equiv \langle v_j|T^p|v_j\rangle$. For $j = 1$, $A_1^{(p)} = C(pa)/C(0)$; by definition $B_1^{(p)} = 0$. The recursion relations

$$A_{j+1}^{(p)} = \frac{1}{\beta_{j+1}^2}\Big[A_j^{(p+2)} + \alpha_j^2 A_j^{(p)} + \beta_j^2 A_{j-1}^{(p)} - 2\alpha_j A_j^{(p+1)} + 2\alpha_j\beta_j B_j^{(p)} - 2\beta_j B_j^{(p+1)}\Big] \tag{7}$$

and

$$B_{j+1}^{(p)} = \frac{1}{\beta_{j+1}}\left[A_j^{(p+1)} - \alpha_j A_j^{(p)} - \beta_j B_j^{(p)}\right] \tag{8}$$

provide matrix elements for $j > 1$, where $p \in \{1, \ldots 2(m-j)+1\}$, $\alpha_j = A_j^{(1)}$, $\beta_1 = B_1^{(p)} = 0$, and $\beta_{j+1} = \sqrt{A_j^{(2)} - \alpha_j^2 - \beta_j^2} = B_{j+1}^{(1)}$. Similar recursions are discussed for Monte Carlo thermalization times in Ref. [67].

These recursions provide the nonzero matrix elements $T_{ii}^{(m)} = A_i^{(1)} = \alpha_i$ and $T_{i(i+1)}^{(m)} = T_{(i+1)i}^{(m)} = B_{i+1}^{(1)} = \beta_{i+1}$. The $m \times m$ matrix $T_{ij}^{(m)}$ can be diagonalized straightforwardly to provide $\lambda_k^{(m)}$ and $E_k^{(m)} \equiv -(1/a)\ln \lambda_k^{(m)}$ with $k \in \{1, \ldots, m\}$. The $m = 1$ case simplifies to $T_{11}^{(1)} = \alpha_1 = C(a)/C(0)$ and therefore $E_0^{(1)} = E(a)$.

The recursion relations shown here are applicable to any $C(t)$ admitting a spectral representation; see Supplemental Material for a proof. They further apply to stochastic estimates of $C(t)$ if $T_{ij}^{(m)} \in \mathbb{C}$ is permitted [68], and they are interpreted as applying oblique Lanczos [70–72] with a non-Hermitian transfer matrix $T^{(m)}$ that exactly describes $C(t)$ at finite statistics, as proven in Ref. [73]. Unless stated otherwise, theoretical results below assume that $T^{(m)}$ is Hermitian and therefore only apply exactly at infinite statistics and stochastically at finite statistics.

Convergence—Cauchy's interlacing theorem guarantees that $\lambda_k^{(m)}$ provides a lower bound on λ_k [33,52,74]. Therefore $E_k^{(m)}$ provides a variational upper bound on E_k. The KPS bound [51–53] further constrains the approximation errors of ground-state Ritz values,

$$\frac{\lambda_0 - \lambda_0^{(m)}}{\lambda_0} \leq \left[\frac{\tan \arccos Z_0}{T_{m-1}(2e^{\delta} - 1)}\right]^2, \tag{9}$$

where the $T_k(x)$ are Chebyshev polynomials of the first kind, $T_k(\cos x) = \cos(kx)$. For large k, $T_k(x) \approx \frac{1}{2}(x + \sqrt{x^2 - 1})^k$, and the KPS bound simplifies to

$$\frac{\lambda_0 - \lambda_0^{(m)}}{\lambda_0} \lesssim \frac{4(1 - Z_0^2)}{Z_0^2} \times \begin{cases} e^{-2(m-1)\delta} & \delta \gg 1 \\ e^{-4(m-1)\sqrt{\delta}} & \delta \ll 1 \end{cases}. \tag{10}$$

For large δ, this resembles the $O(e^{-(t/a)\delta})$ asymptotic error of the effective mass (power-iteration method) with $t/a \propto 2m$. For small δ, Lanczos converges exponentially faster than the power-iteration method because $\sqrt{\delta} \gg \delta$. The latter region is the relevant one near the continuum limit where $\delta = a(E_1 - E_0) \ll 1$.

Figure 1 compares the practical convergence of $E_0^{(m)}$ with that of $E(t)$ for a 20-state correlation-function model defined by Eq. (2) with $Z_n = (n+1)$ and $aE_n = 0.1(n+1)$ for $n = 0, \ldots, 19$. The Ritz values exactly reproduce the complete energy spectrum after 20 iterations and for the ground state are 5 orders of magnitude more accurate than the standard effective mass after 12 iterations.

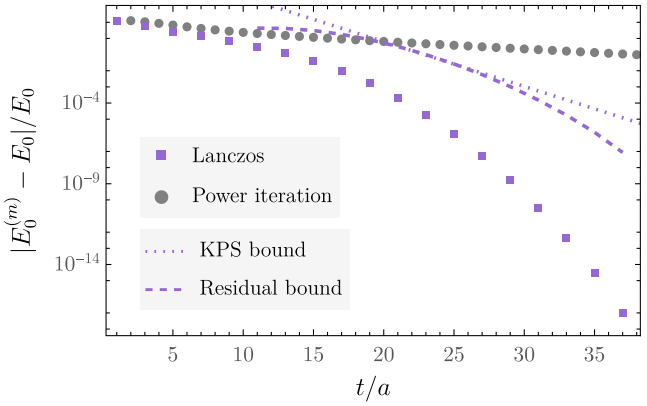


FIG. 1. Relative errors of Lanczos and power-iteration (effective mass) applied to $\{C(0), \ldots, C(ta)\}$ versus $t/a = 2m - 1$ for the 20-state mock data described in the main text (including the trivial extension of power-iteration to half-integer m). The Kaniel-Paige-Saad bound, Eq. (9), is shown as a dotted line. The residual bound, Eq. (11), is shown as a dashed line for $m \geq 6$ ($E_0^{(m)}$ is closer to E_n with $n > 0$ for smaller m).

Remarkably, it is also possible to bound the difference between $E_k^{(m)}$ and an exact energy in terms of directly calculable quantities [33,35]. The approximation error of T in the Lanczos basis is the residual norm β_{m+1} by Eq. (6), and the change of basis relating this to the Ritz basis is provided by the eigenvectors $\omega_n^{(m)}$ of $T_{ij}^{(m)}$. The residual bound states that for any Ritz value $\lambda_k^{(m)}$ there exists an eigenvalue λ of T satisfying

$$\min_{\lambda \in \{\lambda_n\}} |\lambda_k^{(m)} - \lambda|^2 \leq B_k^{(m)} \equiv |\beta_{m+1}|^2 |\omega_{mk}^{(m)}|^2 V_k^{(m)}, \tag{11}$$

where $\omega_{jk}^{(m)}$ denotes the j th component of $\omega_k^{(m)}$. Here, $V_k^{(m)} \equiv \langle v_{m+1}|v_{m+1}\rangle / \langle y_k^{(m)}|y_k^{(m)}\rangle$ involves the Ritz vectors $|y_n^{(m)}\rangle \equiv \sum_j |v_j^{(m)}\rangle \omega_{jn}^{(m)}$ and is equal to unity when $T_{ij}^{(m)}$ is Hermitian. Importantly, the residual bound does not assume Hermiticity of $T^{(m)}$. Its evaluation in the context of oblique Lanczos is detailed in Supplemental Material. Note that it is not guaranteed that $\lambda_k^{(m)}$ is close to λ_k—eigenvectors that have sufficiently small overlap with $|\psi\rangle$ can be "missed" by Lanczos [33,65,75]—but a two-sided systematic uncertainty interval in which an eigenvalue of T is guaranteed to exist can be computed for each $\lambda_k^{(m)}$. This is a significant advantage over standard methods, which can also miss energy eigenstates in practice [11,76–78] and for finite t only have one-sided systematic uncertainty bounds arising from the variational principle.

It is noteworthy that an improved estimator based on Prony's method [27–31] gives results that are numerically identical to the $\lambda_k^{(m)}$ when applied to the $2m$ correlation-function values $\{C(0), \ldots, C[(2m-1)a]\}$. After this work was completed, this and further coincidences between

Lanczos and other methods were explored [79,80] and placed in the context of a larger equivalence class [81]. Here, I focus on important properties of the $\lambda_k^{(m)}$—including the KPS and residual bounds discussed above, as well as methods for filtering between physical and spurious Ritz values in applications to noisy data discussed below—that can be derived from their Lanczos definitions and are not obvious from the perspective of Prony's method [82].

Numerical stability—Numerical artifacts in Lanczos arising from finite-precision arithmetic have been studied in detail and result in "spurious eigenvalues" that do not converge toward definite values as well as multiple copies of genuine eigenvalues [33,52,83,84]. A simple yet effective [46,85] method for filtering spurious eigenvalues was introduced by Cullum and Willoughby (CW) [83,84]. This method is based on the nontrivial realization that large differences between Ritz values and T eigenvalues can only arise for a nondegenerate eigenvalue when $\lambda_n^{(m)}$ is also an eigenvalue of the matrix $\tilde{T}_{ij}^{(m)}$ defined by deleting the first row and column of $T_{ij}^{(m)}$ [83,84].

The threshold for when the distance $d_k^{(m)}$ between an eigenvalue of $T_{ij}^{(m)}$ and the nearest eigenvalue of $\tilde{T}_{ij}^{(m)}$ should be considered zero—and thus the eigenvalue spurious—is obvious in fixed-precision Lanczos applications without statistical noise [83,84] but for Monte Carlo results it depends on statistical precision. Since spurious eigenvalues appear because of statistical fluctuations and do not converge to definite values, the distribution of Ritz values $\lambda_k^{(b,m)}$ obtained using bootstrap resampling [86,88–90] with $b \in \{1, \ldots, N_{\text{boot}}\}$ is useful for identifying a threshold ε_{CW} for which eigenvalues with $d_k^{(m)} < \varepsilon_{\text{CW}}$ are deemed spurious as described below.

This construction does an imperfect job of filtering between spurious and nonspurious eigenvalues in the presence of noise. Using outlier-robust bootstrap statistics, in particular the bootstrap median and its empirical bootstrap confidence intervals, can mitigate the statistical noise that results from misidentification.

Lanczos estimates for E_0 are therefore obtained using the following steps: (1) compute the Ritz values $\lambda_k^{(b,m)}$ for N_{boot} bootstrap samples using Lanczos recursions, Eqs. (7), (8). If $|\arg \lambda_k^{(b,m)}| > \varepsilon_{\text{float}} \sim 10^{-12}$, discard as spurious. (2) Place the Cullum-Willoughby threshold, ε_{CW}, below all $\ln d^{(b,m)}$ histogram bins with $O(N_{\text{boot}} m)$ counts [87]. If $d_k^{(b,m)} > \varepsilon_{\text{CW}}$, discard as spurious. (3) $E_0 = -\ln \text{median}_b[\lambda_0^{(b,m_{\text{max}})}]$, where $\lambda_0^{(b,m)}$ is the largest nonspurious $\lambda_k^{(b,m)}$ less than one and $m_{\text{max}} = (\beta - 1)/2$ is the largest m where $B_k^{(b,m)}$ is computable. (4) To compute uncertainties, use a nested resampling procedure wherein, for each "outer" bootstrap ensemble, the median is taken over estimates computed on N_{boot} "inner" bootstrap ensembles drawn from the outer one. Empirical confidence intervals of the outer bootstrap results provide (idiomatic) bootstrap uncertainties for E_0.

Lanczos estimates for B_0 are computed from $B_k^{(b,m_{\text{max}})}$ using an identical nested bootstrap procedure.

Simple harmonic oscillator—Complex scalar field theory in $(0+1)D$ with periodic boundary conditions, $\varphi(\beta) = \varphi(0)$, and the action

$$S = a \sum_{t=0}^{\beta-1} \{\varphi(t)^* [\varphi(t+a) - 2\varphi(t) + \varphi(t-a)] \frac{1}{a^2} + (aM)^2 |\varphi(t)|^2\} \tag{12}$$

describes a system of noninteracting bosons with mass aM at temperature $1/\beta$. For $\beta \to \infty$ it is equivalent to a pair of simple harmonic oscillators. The theory has a U(1) symmetry $\varphi \to e^{i\theta}\varphi$ whose conserved charge Q corresponds to φ particle number. Correlation functions for systems with charge Q have ground-state energies Qm. Since $|\varphi|^2$ has $Q = 0$, the variances of charge Q correlation functions are asymptotically constant. This gives calculations of $Q = 1$ correlation functions an exponentially severe SNR problem that is similar to the SNR problem facing baryons in LQCD [91,92].

A correlation function with $Q = 1$ that has overlap with both ground and excited states can be defined as

$$C_\varphi(t) \equiv \langle \varphi(t) |\varphi(t)|^{3/2} \varphi(0)^* |\varphi(0)|^{3/2} \rangle. \tag{13}$$

Results for $E(t)$ and $E_0^{(m)}$ are shown in Fig. 2 for an ensemble of 10^4 field configurations with $aM = 0.1$ and $\beta/a = 100$, where $C_\varphi(t)$ is averaged over all translations of the origin. Blocking analysis shows that averaging over $N_{\text{block}} = 10$ configurations is sufficient to provide negligible autocorrelations. Uncertainties are calculated using (nested) bootstrap confidence intervals with $N_{\text{boot}} = 200$.

Lanczos results converge within uncertainties to the exact result $aE_0 \approx 0.099\,96$ after $m = 3$ iterations, corresponding

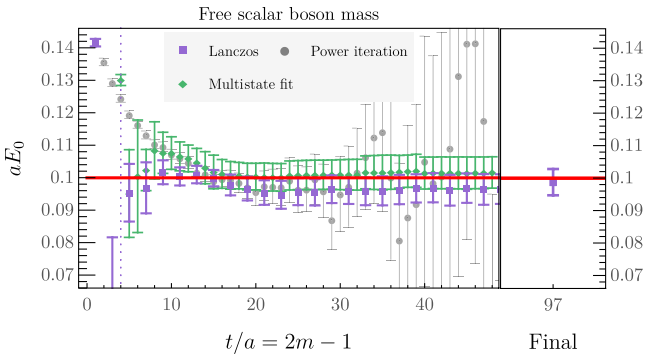


FIG. 2. Lanczos results for E_0 are compared with power-iteration (effective mass) results after m iterations as a function of the maximum $t/a = 2m - 1$ for which $C(t)$ is included. Multistate fit results are shown as functions of the maximum t for which $C(t)$ is included. The exact result is a red line.

to $t/a = 5$, while $E(t)$ reaches similar convergence for $t/a \sim 10$. Further, $E_0^{(m)}$ converges to the true ground-state energy even in the presence of thermal states, as proven in Supplemental Material, and Lanczos results remain consistent with aM for $t > \beta/2$. The Lanczos SNR also converges to a constant value for large m. This is very different from the power-iteration (effective-mass) SNR, which decreases exponentially according to Parisi-Lepage scaling. In this way Lanczos SNR scaling offers the same improved SNR scaling of multistate fit results as a function of the maximum time t_{max} included in fits.

Applying Lanczos for the full $m_{\text{max}} = (\beta - 1)/2 = 49$ iteration count available gives $E_0^{(m_{\text{max}})} = 0.0987(40)$. The two-sided window provided by the residual bound is $[0.065(12), 0.128(10)]$, where $-\ln(\lambda_k^{(m)} \pm B_k^{(m)})$ is computed for the m where $B_k^{(m)}$ is minimized and uncertainties correspond to bootstrap empirical confidence intervals for $-\ln\left(\lambda_k^{(b,m)} \pm \sqrt{B_k^{(b,m)}}\right)$. This window is an order of magnitude larger than the statistical uncertainty of $E_0^{(m_{\text{max}})}$ but nonetheless provides a meaningful constraint on the possible size of excited-state effects. Since the minimum $B_k^{(m)} = 0.000\,83(69)$ is not clearly resolved from zero, the scaling of the size of this two-sided residual-bound window with statistical ensemble size N is nontrivial and important to explore in future work.

This can be compared to standard multistate fits to $C_\varphi(t)$ using the methodology for averaging over t_{min} and choosing N_{states} detailed in Refs. [11,93]: a weighted average of multistate fits with all $t_{\text{min}}/a \geq 1$ gives 0.1016(52). Lanczos and this weighted average both agree with the exact result within 1σ; the Lanczos uncertainties are ≈30% smaller. Here, as in many LQCD applications, the sample covariance matrix is ill-conditioned; I regulate it using linear shrinkage [94] as in Ref. [95]. Several other choices are required to precisely define the fitting scheme: N_{states} for each fit range is chosen using the Akaike information criterion (AIC) [96] using $\text{tol}_{AIC} = -0.5$ [93], only fit ranges with at least $t_{\text{plateau}} = 6$ [93] points are included, and numerical checks on optimizer convergence are implemented as in Ref. [93]. Both Lanczos and multistate fit results converge to the exact ground-state energy within 1σ for $t_{\text{max}}/a \sim 2m - 1 \sim 5$, as long as one-state fits to short time ranges are excluded ($t_{\text{plateau}} \geq 5$).

Fits with small t_{min} can be inaccurate even when $\chi^2/\text{d.o.f.} < 1$: one-state fits with $t_{\text{min}} = 7$ and $t_{\text{max}} = 35$ (chosen via SNR cutoff [93]) give 0.1079(17), a 4σ discrepancy, with $\chi^2/\text{d.o.f.} = 0.74$. This underscores the importance of the residual bound, which is rigorously valid even for small m. As an extreme case, $E_0^{(1)} = 0.1416(12)$ has clearly not converged within uncertainties, but $B_0^{(1)} = 0.0045(3)$ still provides a two-sided window $[0.0672(26), 0.2219(34)]$ that includes the true ground-state energy.

Lattice QCD—Correlation functions for baryons and nuclei in LQCD have exponential SNR problems that can make it difficult to isolate ground states. To test the accuracy and precision of Lanczos methods for baryons, I computed proton correlation functions $C_p(t) = \langle p(t)\bar{p}(0)\rangle$ using pointlike proton interpolating operators $p(x) = u^T(x)C\gamma_5 d(x)(1+\gamma_4)d(x)$ projected to zero spatial momentum for 64 sources on a single time slice of 76 gauge-field configurations with $L/a = 48$, $\beta/a = 96$, and $N_f = 2+1$ dynamical quarks with light quark masses corresponding to $m_\pi \approx 170$ MeV and $a \approx 0.091(1)$ fm [97,98]. The action corresponds to the Lüscher-Weisz gauge action [99] and clover-improved [100] Wilson fermion action with one step of stout smearing [101]; a Hermitian transfer matrix representation is therefore only valid for low-energy states [58]. Results for $C(t)$ and $C(-t)$ are averaged. Autocorrelations are found to be negligible via blocking analysis.

Lanczos results give $E_0^{(m_{\text{max}})} = 0.429(20)$ for $m_{\text{max}} = 47$ as shown in Fig. 3; see Supplemental Material for more details and pion results. The two-sided residual-bound window is $[0.350(31), 0.523(26)]$. A high-statistics

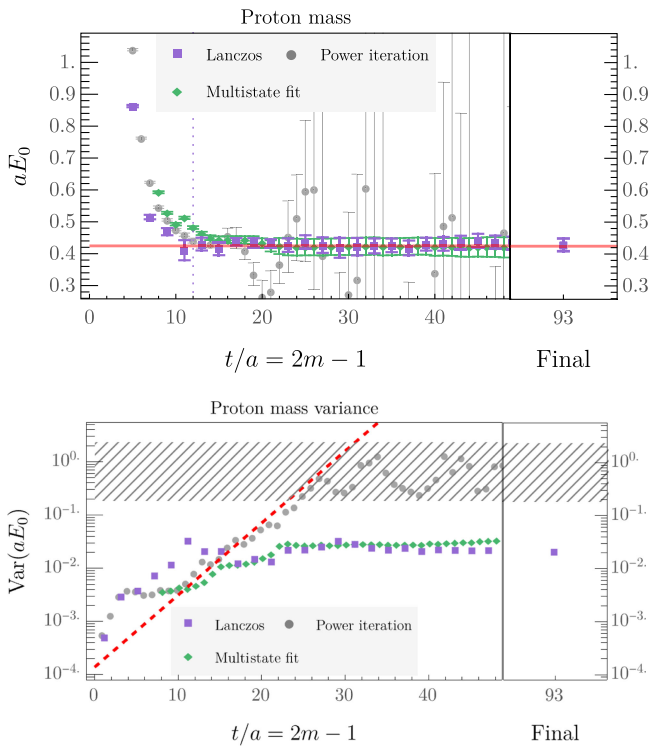


FIG. 3. Top: Proton $E(t)$, $E_0^{(m)}$, and multistate fit results. aM_N^{big} is shown as a red band; other details are as in Fig. 2. Bottom: variances compared with Parisi-Lepage scaling $\propto e^{(M_N - \frac{3}{2}m_\pi)t}$ [14,15] (red dashed line). Hatching indicates the noise region where SNR ≤ 1 and variance estimates may be unreliable, which ranges from $\text{Var}E_0^{(m)} = [E_0^{(m)}]^2$ to the finite-statistics variance limit $N_{\text{src}}\text{Var}E(a)$ [91], where assuming negligible autocorrelations $N_{\text{src}} = 64 \times 76$.

benchmark is provided by model-averaged fits to correlation functions computed by the NPLQCD Collaboration using the same action with $N_{\rm cfg} = 670$ and 512 Gaussian-smeared sources per configuration: $aM_N^{\rm big} = 0.4244(44)$. Lanczos results agree within 1σ.

Two-state fits to $C_p(t)$ with $t_{\rm min}/a = 11$ give 0.4383(86) with $\chi^2/\text{d.o.f.} = 0.71$. A weighted average of multistate fits with all $t_{\rm min}/a \geq 2$ using the strategy in Refs. [11,93] gives 0.443(12). These are 1.5σ and 1.6σ larger than $aM_N^{\rm big}$, respectively. For very large $t_{\rm max} \in [25, 48]$, multistate fits give accurate results 0.420(30) with larger uncertainties. Lanczos energy estimators converge to exact results within 1σ for $2m - 1 \gtrsim 11$, while multistate fit weighted averages (with $t_{\rm plateau} \geq 5$ [93] to exclude short one-state fits) do not converge to $M_N^{\rm big}$ within 1σ until $t_{\rm max} \gtrsim 20$. For $11 \lesssim t_{\rm max}/a \lesssim 20$, multistate fits show $\geq 1\sigma$ signals of bias, effective-mass results have large uncertainties that appear non-Gaussian, while Lanczos results achieve negligible bias with comparable variance to multistate fit results.

The variance of $E_0^{(m)}$ is shown in Fig. 3. It approaches an $O(10^{-2})$ constant for $t/a \gtrsim 20$ with qualitatively similar behavior to the multistate fit variance. This is in contrast to power-iteration and effective-mass results, whose correlations do not saturate and variance grows exponentially with Parisi-Lepage scaling. Lanczos therefore provides an algebraic estimator that is free from exponential SNR degradation. Perhaps relatedly, correlations $\text{Corr}[E_0^{(m)}, E_0^{(m')}] \sim [0.5, 1]$ are visible for $m, m' \gtrsim 20$ that suggest Lanczos results using bootstrap median estimators are relatively insensitive to $C(t)$ with $t/a \gtrsim 40$. Significant large-m correlations are specific to bootstrap-median Lanczos estimators; sample-mean estimators have smaller correlations but larger variance as shown in Supplemental Material. In both cases, Lanczos energy estimators avoid the finite-sample bias seen in very large-t power-iteration and effective-mass results, for which the variance is bounded to be $\geq 1/N$ times the variance of $E(a)$ due to circular statistics [102] of correlation-function phases and $\text{Re}E(t) \to \frac{3}{2} m_\pi$ in the $t \to \infty$ limit at finite N [91].

Discussion—The method for applying the Lanczos algorithm to infinite-dimensional transfer matrices introduced here provides accurate predictions for simple harmonic oscillator and LQCD ground-state energies. In particular, Lanczos achieves higher accuracy and similar precision to multistate fits involving small imaginary times. A two-sided error bound further shows excited-state effects cannot shift Lanczos results far outside their statistical uncertainties. Challenges arise from spurious eigenvalues, but an implementation of the Cullum-Willoughby test using bootstrap histograms and bootstrap median estimators mitigate their effects in these examples. Future refinements improving the robustness of spurious eigenvalue removal could improve the statistical precision of Lanczos energy results and residual bounds.

In conclusion, Lanczos provides rapidly convergent algebraic energy estimators without SNR problems and two-sided bounds on excited-state effects that could be useful for a wide range of hadron spectroscopy calculations where isolating ground states is challenging, including studies of nucleon, nuclear, and highly boosted systems. The existence of two-sided bounds on Lanczos energy estimates using a finite number of $C(t)$ points provides a qualitative improvement over the one-sided bounds available to variational methods and could have wide-ranging applications.

Acknowledgments—I thank Dan Hackett, Ryan Abbot, Benoît Assi, Zohreh Davoudi, Will Detmold, George Fleming, Dorota Grabowska, Anthony Grebe, Marc Illa, Will Jay, Andreas Kronfeld, Assumpta Parreño, Robert Perry, Dimitra Pefkou, Fernando Romero-López, Martin Savage, Phiala Shanahan, and Ruth Van de Water for stimulating discussions and helpful comments. This manuscript has been authored by FermiForward Discovery Group, LLC under Contract No. 89243024CSC000002 with the U.S. Department of Energy, Office of Science, Office of High Energy Physics. This research used facilities of the USQCD Collaboration, which are funded by the Office of Science of the U.S. Department of Energy. The Chroma [103], QUDA [104–106], and QDP-JIT [107] software libraries were used in this work.

Data availability—The data supporting this study's findings are available within the article.

[1] Y.-C. Jang, R. Gupta, B. Yoon, and T. Bhattacharya, Axial vector form factors from lattice QCD that satisfy the PCAC relation, Phys. Rev. Lett. **124**, 072002 (2020).
[2] G. S. Bali, L. Barca, S. Collins, M. Gruber, M. Löffler, A. Schäfer, W. Söldner, P. Wein, S. Weishäupl, and T. Wurm (RQCD Collaboration), Nucleon axial structure from lattice QCD, J. High Energy Phys. 05 (2020) 126.
[3] C. Alexandrou *et al.*, Nucleon axial and pseudoscalar form factors from lattice QCD at the physical point, Phys. Rev. D **103**, 034509 (2021).
[4] S. Park, R. Gupta, B. Yoon, S. Mondal, T. Bhattacharya, Y.-C. Jang, B. Joó, and F. Winter (Nucleon Matrix Elements (NME) Collaboration), Precision nucleon charges and form factors using $(2+1)$-flavor lattice QCD, Phys. Rev. D **105**, 054505 (2022).
[5] D. Djukanovic, G. von Hippel, J. Koponen, H. B. Meyer, K. Ottnad, T. Schulz, and H. Wittig, Isovector axial form factor of the nucleon from lattice QCD, Phys. Rev. D **106**, 074503 (2022).
[6] Y.-C. Jang, R. Gupta, T. Bhattacharya, B. Yoon, and H.-W. Lin (Precision Neutron Decay Matrix Elements (PNDME) Collaboration), Nucleon isovector axial form factors, Phys. Rev. D **109**, 014503 (2024).

[7] C. Alexandrou, S. Bacchio, M. Constantinou, J. Finkenrath, R. Frezzotti, B. Kostrzewa, G. Koutsou, G. Spanoudes, and C. Urbach (Extended Twisted Mass), Nucleon axial and pseudoscalar form factors using twisted-mass fermion ensembles at the physical point, Phys. Rev. D **109**, 034503 (2024).

[8] R. Gupta, Isovector axial charge and form factors of nucleons from lattice QCD, Proc. Sci., LATTICE2023 (**2024**) 124.

[9] A. Francis, J. R. Green, P. M. Junnarkar, C. Miao, T. D. Rae, and H. Wittig, Lattice QCD study of the H dibaryon using hexaquark and two-baryon interpolators, Phys. Rev. D **99**, 074505 (2019).

[10] B. Hörz *et al.*, Two-nucleon S-wave interactions at the $SU(3)$ flavor-symmetric point with $m_{ud} \simeq m_s^{\mathrm{phys}}$: A first lattice QCD calculation with the stochastic Laplacian Heaviside method, Phys. Rev. C **103**, 014003 (2021).

[11] S. Amarasinghe, R. Baghdadi, Z. Davoudi, W. Detmold, M. Illa, A. Parreño, A. V. Pochinsky, P. E. Shanahan, and M. L. Wagman, Variational study of two-nucleon systems with lattice QCD, Phys. Rev. D **107**, 094508 (2023).

[12] J. R. Green, A. D. Hanlon, P. M. Junnarkar, and H. Wittig, Weakly bound H dibaryon from SU(3)-flavor-symmetric QCD, Phys. Rev. Lett. **127**, 242003 (2021).

[13] W. Detmold, M. Illa, W. I. Jay, A. Parreño, R. J. Perry, P. E. Shanahan, and M. L. Wagman, Constraints on the finite volume two-nucleon spectrum at $m_\pi \approx 806$ MeV, arXiv:2404.12039.

[14] G. Parisi, The strategy for computing the hadronic mass spectrum, Phys. Rep. **103**, 203 (1984).

[15] G. P. Lepage, The analysis of algorithms for lattice field theory, in Theoretical Advanced Study Institute in Elementary Particle Physics (1989).

[16] S. R. Beane, W. Detmold, T. C. Luu, K. Orginos, A. Parreño, M. J. Savage, A. Torok, and A. Walker-Loud (NPLQCD Collaboration), High statistics analysis using anisotropic clover lattices: (II) Three-baryon systems, Phys. Rev. D **80**, 074501 (2009).

[17] S. R. Beane, W. Detmold, H.-W. Lin, T. C. Luu, K. Orginos, M. J. Savage, A. Torok, and A. Walker-Loud (NPLQCD Collaboration), High statistics analysis using anisotropic clover lattices: (III) baryon-baryon interactions, Phys. Rev. D **81**, 054505 (2010).

[18] Z. Davoudi, W. Detmold, K. Orginos, A. Parreño, M. J. Savage, P. Shanahan, and M. L. Wagman, Nuclear matrix elements from lattice QCD for electroweak and beyond-standard-model processes, Phys. Rep. **900**, 1 (2021).

[19] G. Fox, R. Gupta, O. Martin, and S. Otto, Monte Carlo estimates of the mass gap of the O(2) and O(3) spin models in $(1+1)$-dimensions, Nucl. Phys. **B205**, 188 (1982).

[20] C. Michael and I. Teasdale, Extracting glueball masses from lattice QCD, Nucl. Phys. **B215**, 433 (1983).

[21] M. Lüscher and U. Wolff, How to calculate the elastic scattering matrix in two-dimensional quantum field theories by numerical simulation, Nucl. Phys. **B339**, 222 (1990).

[22] B. Blossier, M. Della Morte, G. von Hippel, T. Mendes, and R. Sommer, On the generalized eigenvalue method for energies and matrix elements in lattice field theory, J. High Energy Phys. 04 (2009) 094.

[23] G. T. Fleming, Beyond generalized eigenvalues in lattice quantum field theory, in *40th International Symposium on Lattice Field Theory* (2023), arXiv:2309.05111.

[24] R. A. Briceno, J. J. Dudek, and R. D. Young, Scattering processes and resonances from lattice QCD, Rev. Mod. Phys. **90**, 025001 (2018).

[25] J. Bulava *et al.*, Hadron spectroscopy with lattice QCD, in Snowmass 2021 (2022), arXiv:2203.03230.

[26] A. D. Hanlon, Hadron spectroscopy and few-body dynamics from lattice QCD, Proc. Sci., LATTICE2023 (**2024**) 106 [arXiv:2402.05185].

[27] G. T. Fleming, What can lattice QCD theorists learn from NMR spectroscopists?, *in 3rd International Workshop on Numerical Analysis and Lattice QCD* (2004), pp. 143–152, arXiv:hep-lat/0403023.

[28] H.-W. Lin and S. D. Cohen, Lattice QCD beyond ground states, *in 4th International Workshop on Numerical Analysis and Lattice QCD* (2007).

[29] G. T. Fleming, S. D. Cohen, H.-W. Lin, and V. Pereyra, Excited-state effective masses in lattice QCD, Phys. Rev. D **80**, 074506 (2009).

[30] S. R. Beane, W. Detmold, T. C. Luu, K. Orginos, A. Parreno, M. J. Savage, A. Torok, and A. Walker-Loud, High statistics analysis using anisotropic clover lattices: (I) Single hadron correlation functions, Phys. Rev. D **79**, 114502 (2009).

[31] M. Fischer, B. Kostrzewa, J. Ostmeyer, K. Ottnad, M. Ueding, and C. Urbach, On the generalised eigenvalue method and its relation to Prony and generalised pencil of function methods, Eur. Phys. J. A **56**, 206 (2020).

[32] C. Lanczos, An iteration method for the solution of the eigenvalue problem of linear differential and integral operators, J. Res. Natl. Bur. Stand. B **45**, 255 (1950).

[33] B. Parlett, The Symmetric Eigenvalue Problem, Classics in Applied Mathematics (Society for Industrial and Applied Mathematics, Philadelphia, 1980).

[34] G. H. Golub and D. P. O'Leary, Some history of the conjugate gradient and Lanczos algorithms: 1948–1976, SIAM Rev. **31**, 50 (1989).

[35] B. N. Parlett, Do we fully understand the symmetric Lanczos algorithm yet (1995), https://apps.dtic.mil/sti/citations/tr/ADA289614.

[36] G. Meurant and Z. Strakoš, The Lanczos and conjugate gradient algorithms in finite precision arithmetic, Acta Numer., **15**, 471 (2006).

[37] Y. Saad, Numerical Methods for Large Eigenvalue Problems: Revised Edition, Classics in Applied Mathematics (Society for Industrial and Applied Mathematics, Philadelphia, 2011).

[38] G. H. Golub and C. F. Van Loan, *Matrix Computations* (Johns Hopkins University Press, Philadelphia, PA, 2013).

[39] V. Hernandez, J. E. Roman, A. Tomas, and V. Vidal, A survey of software for sparse eigenvalue problems, Technical Report STR-5, Universitat Politècnica de València, 2006, available at https://slepc.upv.es.

[40] M. Caffarel, F. X. Gadea, and D. M. Ceperley, Lanczós-type algorithm for quantum Monte Carlo data, Europhys. Lett. **16**, 249 (1991).

[41] S. Sorella, Generalized Lanczos algorithm for variational quantum Monte Carlo, Phys. Rev. B **64**, 024512 (2001).

[42] F. Becca and S. Sorella, *Quantum Monte Carlo Approaches for Correlated Systems* (Cambridge University Press, Cambridge, England, 2017).

[43] I. M. Barbour, P. Gibbs, J. P. Gilchrist, H. Schneider, G. Schierholz, and M. Teper, Strong evidence for spontaneous chiral symmetry breaking in (quenched) QCD, Phys. Lett. B **136**, 80 (1984).

[44] I. M. Barbour, N. E. Behilil, P. E. Gibbs, G. Schierholz, and M. Teper, THE Lanczos method in lattice gauge theories (1984), https://inspirehep.net/literature/204843.

[45] I. M. Barbour, N. E. Behilil, P. E. Gibbs, M. Rafique, K. J. M. Moriarty, and G. Schierholz, Updating fermions with the Lanczos method, J. Comput. Phys. **68**, 227 (1987).

[46] T. Kalkreuter, Study of Cullum's and Willoughby's Lanczos method for Wilson fermions, Comput. Phys. Commun. **95**, 1 (1996).

[47] A. D. Kennedy, I. Horvath, and S. Sint, A New exact method for dynamical fermion computations with nonlocal actions, Nucl. Phys. B, Proc. Suppl. **73**, 834 (1999).

[48] M. A. Clark, C. Jung, and C. Lehner, Multi-grid Lanczos, EPJ Web Conf. **175**, 14023 (2018).

[49] H. Jeong, C. DeTar, and S. Gottlieb, Performance of several Lanczos eigensolvers with HISQ fermions, *Proc. Sci.*, LATTICE2021 (2022) 053 [arXiv:2201.03755].

[50] J. B. Kogut and L. Susskind, Hamiltonian formulation of Wilson's lattice gauge theories, Phys. Rev. D **11**, 395 (1975).

[51] S. Kaniel, Estimates for some computational techniques in linear algebra, Math. Comput. **20**, 369 (1966).

[52] C. C. Paige, The computation of eigenvalues and eigenvectors of very large sparse matrices, Ph.D.thesis, London University, London, UK, 1971.

[53] Y. Saad, On the rates of convergence of the Lanczos and the block-Lanczos methods, SIAM J. Num. Anal. **17**, 687 (1980).

[54] M. Della Morte and L. Giusti, Exploiting symmetries for exponential error reduction in path integral Monte Carlo, Comput. Phys. Commun. **180**, 813 (2009).

[55] M. Della Morte and L. Giusti, Symmetries and exponential error reduction in Yang-Mills theories on the lattice, Comput. Phys. Commun. **180**, 819 (2009).

[56] M. Della Morte and L. Giusti, A novel approach for computing glueball masses and matrix elements in Yang-Mills theories on the lattice, J. High Energy Phys. 05 (2011) 056.

[57] M. Lüscher, Construction of a selfadjoint, strictly positive transfer matrix for euclidean lattice gauge theories, Commun. Math. Phys. **54**, 283 (1977).

[58] M. Lüscher and P. Weisz, Definition and general properties of the transfer matrix in continuum limit improved lattice gauge theories, Nucl. Phys. **B240**, 349 (1984).

[59] See Supplemental Material, which includes Refs. [60,61], at http://link.aps.org/supplemental/10.1103/pcvc-734h for additional details on the implementation of the Lanczos algorithm used to compute the results of the main text, including thermal effects, the Cullum-Willoughby test, oblique Lanczos recursion relations, residual bounds, and correlations.

[60] D. C. Hackett, P. R. Oare, D. A. Pefkou, and P. E. Shanahan, Gravitational form factors of the pion from lattice QCD, Phys. Rev. D **108**, 114504 (2023).

[61] R. Abbott, W. Detmold, M. Illa, A. Parreño, R. J. Perry, F. Romero-López, P. E. Shanahan, and M. L. Wagman, QCD constraints on isospin-dense matter and the nuclear equation of state, Phys. Rev. Lett. **134**, 011903 (2025).

[62] R. V. Mises and H. Pollaczek-Geiringer, Praktische Verfahren der Gleichungsauflösung, Z. Angew. Math. Mech. **9**, 58 (1929).

[63] B. N. Parlett, H. Simon, and L. M. Stringer, On estimating the largest eigenvalue with the Lanczos algorithm, Math. Comput. **38**, 153 (1982).

[64] J. Kuczyński and H. Woźniakowski, Estimating the largest eigenvalues by the power and Lanczos algorithms with a random start, SIAM J. Matrix Anal. Appl. **13**, 1094 (1992).

[65] A. B. J. Kuijlaars, Which eigenvalues are found by the Lanczos method?, SIAM J. Matrix Anal. Appl. **22**, 306 (2000).

[66] J. Garza-Vargas and A. Kulkarni, The Lanczos algorithm under few iterations: Concentration and location of the output, SIAM J. Matrix Anal. Appl. **41**, 1312 (2020).

[67] W. DeMeo, A Lanczos procedure for approximating eigenvalues of large stochastic matrices, Ph.D. thesis, 1998.

[68] Nonspurious eigenvalues with $\beta_j^2 \approx 0$ indicate that a Ritz value has converged to an eigenvalue of T; see Refs. [33,35,52,69]. After convergence has been achieved, statistical fluctuations can easily lead to $\beta_j^2 < 0$ and therefore complex $T_{ij}^{(m)}$.

[69] B. N. Parlett and D. S. Scott, The Lanczos algorithm with selective orthogonalization, Math. Comput. **33**, 217 (1979).

[70] Y. Saad, The Lanczos biorthogonalization algorithm and other oblique projection methods for solving large unsymmetric systems, SIAM J. Num. Anal. **19**, 485 (1982).

[71] B. N. Parlett, D. R. Taylor, and Z. A. Liu, A look-ahead Lanczos algorithm for unsymmetric matrices, Math. Comput. **44**, 105 (1985).

[72] N. M. Nachtigal, A look-ahead variant of the Lanczos algorithm and its application to the quasi-minimal residual method for non-Hermitian linear systems, Ph.D. thesis, 1993.

[73] D. C. Hackett and M. L. Wagman, Lanczos for lattice QCD matrix elements, arXiv:2407.21777.

[74] J. H. J. H. Wilkinson, *The Algebraic Eigenvalue Problem*, Monographs on Numerical Analysis (Clarendon Press, Oxford, 1965).

[75] B. Parlett, Misconvergence in the Lanczos algorithm, in Reliable Numerical Commputation (Oxford University Press, New York, 1990).

[76] J. J. Dudek, R. G. Edwards, and C. E. Thomas (Hadron Spectrum Collaboration), Energy dependence of the ρ resonance in $\pi\pi$ elastic scattering from lattice QCD, Phys. Rev. D **87**, 034505 (2013); **90**, 099902(E) (2014).

[77] C. B. Lang and V. Verduci, Scattering in the πN negative parity channel in lattice QCD, Phys. Rev. D **87**, 054502 (2013).

[78] D. J. Wilson, R. A. Briceno, J. J. Dudek, R. G. Edwards, and C. E. Thomas, Coupled $\pi\pi, K\bar{K}$ scattering in P-wave and the ρ resonance from lattice QCD, Phys. Rev. D **92**, 094502 (2015).

[79] J. Ostmeyer, A. Sen, and C. Urbach, On the equivalence of Prony and Lanczos methods for Euclidean correlation functions, Eur. Phys. J. A **61**, 26 (2025).

[80] D. Chakraborty, D. Sood, A. Radhakrishnan, and N. Mathur, Estimating energy levels from lattice QCD correlation functions using a transfer matrix formalism, arXiv:2412.01900.

[81] R. Abbott, D. C. Hackett, G. T. Fleming, D. A. Pefkou, and M. L. Wagman, Filtered Rayleigh-Ritz is all you need, arXiv:2503.17357.

[82] LQCD applications of Prony's method have used fixed m in the range $m \leq 4$ [28–31] and noted that unphysical solutions arising from noise become increasingly common as m is increased [29].

[83] J. Cullum and R. A. Willoughby, Computing eigenvalues of very large symmetric matrices–an implementation of a Lanczos algorithm with no reorthogonalization, J. Comput. Phys. **44**, 329 (1981).

[84] J. K. Cullum and R. A. Willoughby, Lanczos procedures, in *Lanczos Algorithms for Large Symmetric Eigenvalue Computations* Vol. I Theory (Birkhäuser Boston, Boston, MA, 1985), pp. 92–163.

[85] U. Elsner, V. Mehrmann, F. Milde, R. A. Römer, and M. Schreiber, The Anderson model of localization: A challenge for modern eigenvalue methods, SIAM J. Sci. Comput. **20**, 2089 (1999).

[86] B. Efron, *Nonparametric Estimates of Standard Error: The Jackknife, the Bootstrap and Other Methods* (Oxford University Press, New York, 1981), Vol. 68, pp. 589–599.

[87] A precise recipe for defining ϵ_{CW} in terms of three hyperparameters is given in Supplemental Material; examples here use $\Delta = 4$, $K_{\mathrm{CW}} = 3$, and $F_{\mathrm{CW}} = 10$.

[88] A. C. Davison and D. V. Hinkley, The basic bootstraps, in *Bootstrap Methods and their Application, Cambridge Series in Statistical and Probabilistic Mathematics* (Cambridge University Press, Cambridge, England, 1997), pp. 11–69.

[89] P. Young, Everything you wanted to know about data analysis and fitting but were afraid to ask, arXiv:1210.3781.

[90] P. Lepage, C. Gohlke, and D. Hackett, https://github.com/gplepage/gvar (2024).

[91] M. L. Wagman and M. J. Savage, Statistics of baryon correlation functions in lattice QCD, Phys. Rev. D **96**, 114508 (2017).

[92] W. Detmold, G. Kanwar, and M. L. Wagman, Phase unwrapping and one-dimensional sign problems, Phys. Rev. D **98**, 074511 (2018).

[93] S. R. Beane *et al.* (NPLQCD, QCDSF Collaborations), Charged multihadron systems in lattice QCD + QED, Phys. Rev. D **103**, 054504 (2021).

[94] O. Ledoit and M. Wolf, A well-conditioned estimator for large-dimensional covariance matrices, J. Multivariate Anal. **88**, 365 (2004).

[95] E. Rinaldi, S. Syritsyn, M. L. Wagman, M. I. Buchoff, C. Schroeder, and J. Wasem, Lattice QCD determination of neutron-antineutron matrix elements with physical quark masses, Phys. Rev. D **99**, 074510 (2019).

[96] H. Akaike, A new look at the statistical model identification, IEEE Trans. Autom. Control **19**, 716 (1974).

[97] B. Yoon *et al.*, Isovector charges of the nucleon from 2 + 1-flavor QCD with clover fermions, Phys. Rev. D **95**, 074508 (2017).

[98] S. Mondal, R. Gupta, S. Park, B. Yoon, T. Bhattacharya, B. Joó, and F. Winter (Nucleon Matrix Elements (NME) Collaboration), Nucleon momentum fraction, helicity and transversity from 2 + 1-flavor lattice QCD, J. High Energy Phys. 04 (2020) 004.

[99] M. Lüscher and P. Weisz, On-shell improved lattice gauge theories, Commun. Math. Phys. **98**, 433 (1985); **98**, 433(E) (1985).

[100] B. Sheikholeslami and R. Wohlert, Improved continuum limit lattice action for QCD with Wilson fermions, Nucl. Phys. **B259**, 572 (1985).

[101] C. Morningstar and M. J. Peardon, Analytic smearing of SU(3) link variables in lattice QCD, Phys. Rev. D **69**, 054501 (2004).

[102] N. I. Fisher, *Statistical Analysis of Circular Data* (Cambridge University Press, Cambridge, England, 1993).

[103] R. G. Edwards and B. Joó (SciDAC, LHPC, UKQCD Collaborations), The Chroma software system for lattice QCD, Nucl. Phys. B, Proc. Suppl. **140**, 832 (2005).

[104] M. A. Clark, R. Babich, K. Barros, R. C. Brower, and C. Rebbi (QUDA Collaboration), Solving Lattice QCD systems of equations using mixed precision solvers on GPUs, Comput. Phys. Commun. **181**, 1517 (2010).

[105] R. Babich, M. A. Clark, B. Joó, G. Shi, R. C. Brower, and S. Gottlieb (QUDA Collaboration), Scaling lattice QCD beyond 100 GPUs, in International Conference for High Performance Computing, *Networking, Storage and Analysis* (2011), arXiv:1109.2935.

[106] M. A. Clark, B. Joó, A. Strelchenko, M. Cheng, A. Gambhir, and R. C. Brower (QUDA), Accelerating lattice QCD multigrid on GPUs using fine-grained parallelization, in International Conference for High Performance Computing, *Networking, Storage and Analysis* (2016), arXiv:1612.07873.

[107] F. Winter and M.Clark, R. Edwards, and B. Joó, A framework for lattice QCD calculations on GPUs, in *2014 IEEE 28th International Parallel and Distributed Processing Symposium* (2014), pp. 1073–1082.

[108] Wolfram Research Inc., MATHEMATICA, Version 14.0, https://www.wolfram.com/mathematica.

End Matter

Analytic argument for asymptotically constant SNR—The fact that Lanczos SNR approaches a constant at large m can be understood from the perspective of the Lanczos algorithm as a Krylov-space projection method [33]. Explicitly, projection operators can be constructed from the Ritz vectors as $P_n^{(m)} \equiv |y_n^{(m)}\rangle\langle y_n^{(m)}|$ and are related to Ritz values as

$$\lambda_n^{(m)} = \left\langle y_n^{(m)} \middle| T \middle| y_n^{(m)} \right\rangle = \frac{\left\langle \psi \middle| P_n^{(m)} T P_n^{(m)} \middle| \psi \right\rangle}{|\omega_{1n}^{(m)}|^2 \langle \psi|\psi\rangle} \quad \text{(A1)}$$

for a Hermitian subspace of nonspurious Ritz values [73]. $P_n^{(m)}$ converges to the projection operator $P_n \equiv |n\rangle\langle n|$ with finite-m corrections analogous to those appearing the KPS eigenvalue bound, e.g., $P_n^{(m)} = P_n + O(e^{-4m\sqrt{\delta}})$ for $\delta \ll 1$ [33,53,70]. This provides the Hilbert-space operator relation $\psi P_n T P_n \psi^\dagger = |Z_n|^2 e^{-aE_n} |n\rangle\langle n| + O(e^{-4m\sqrt{\delta}})$. At finite statistics, $P_n^{(m)}$ depends on the gauge-field ensemble used and $\psi P_n^{(m)} T P_n^{(m)} \psi^\dagger$ provides an observable whose finite-statistics expectation value coincides with $\lambda_n^{(m)}$. This suggests the variance of $\lambda_n^{(m)}$ is proportional to that of $\psi P_n^{(m)} T P_n^{(m)} \psi^\dagger$ in the limit of large statistics. If the statistical ensemble and m are both large, then $P_n^{(m)}$ approaches P_n and in this limit the variance of $\lambda_n^{(m)}$ is proportional to the variance of the projector $|n\rangle\langle n|$.

The variances of projectors have appealing features including the nonappearance of states with different quantum numbers than the signal squared (e.g., three-pion states in nucleon variances) [54–56]; the finiteness of the variance of $|n\rangle\langle n|$ is already sufficient to ensure the variance of $\lambda_n^{(m)}$ approaches a finite m-independent value. Analogous arguments slow the variance of $\omega_{1n}^{(m)}$ is proportional to that of $\psi P_n^{(m)} \psi^\dagger$ and likewise approaches a constant at large m. The SNR of $E_n^{(m)} = -1/a \ln \lambda_n^{(m)}$ therefore approaches a nonzero constant for large m. This should be contrasted with the power-iteration method, for which $E(2ma)$ is defined by a log ratio of $C(2ma)$ and $C((2m-1)a)$, both of which have zero SNR at large m. Since they are not perfectly correlated, the SNR of $E(2ma)$ vanishes (exponentially) at large m.

Numerical analysis was performed and figures were produced using MATHEMATICA [108].